

Article

Accessibility Study of a Compact Wind Tunnel with an Unequal Spacing Grid for the Outdoor Wind Environment

Xiaojun Ma ¹, Yu Zhao ², Xueying Wen ³ and Jiujiu Chen ^{1,*}¹ College of Biochemical Engineering, Beijing Union University, Beijing 100023, China² Department of Civil and Environmental Engineering, University of Pittsburgh, Pittsburgh, PA 15260, USA³ School of Civil and Resource Engineering, University of Science and Technology Beijing, Beijing 100083, China

* Correspondence: chenjiujiu@buu.edu.cn

Abstract: One of the key issues in architectural design and regional planning is to create a safe and comfortable outdoor building environment, which calls for more studies. Wind tunnel experiments and computational fluid dynamic (CFD) simulations are the primary methods for the current studies. The airflow and boundary conditions are controllable for the wind tunnel experiment, and the data is reliable. In most wind tunnel platforms, spires and roughness elements are applied to create the gradient wind of the atmospheric boundary layer, leading to the oversized, high construction cost, and complex operation. In this paper, in order to explore a simple method for measuring and studying the outdoor building wind environment using wind tunnels, a compact wind tunnel platform adopting grids with unequal spacing was designed and tested, based on the theoretical model of the atmospheric boundary layer. A comparison between the test results and the theoretical values indicated that this new wind tunnel platform could achieve a gradient wind field and is accessible in applying low-speed wind tunnels to the measurement and research of the building wind environment. The application case in a high-rise building of the central business district (CBD) region in Beijing, was presented in this paper. Compared with another analytical method, the CFD simulation, the compact wind tunnel revealed its applicability that could be used for predicting and evaluating the outdoor wind environment around the building. This compact wind tunnel is more flexible and convenient than the traditional ones, with a smaller size, easier construction and operation, and lower costs. Therefore, we suggest more applications of this compact wind tunnel platform in future experimental studies of outdoor wind environments.

Keywords: outdoor wind environment; compact wind tunnel; atmospheric boundary layer; gradient wind



Citation: Ma, X.; Zhao, Y.; Wen, X.; Chen, J. Accessibility Study of a Compact Wind Tunnel with an Unequal Spacing Grid for the Outdoor Wind Environment. *Buildings* **2022**, *12*, 2188. <https://doi.org/10.3390/buildings12122188>

Academic Editors: Yunyang Ye and Xuechen Lei

Received: 13 October 2022

Accepted: 8 December 2022

Published: 9 December 2022

Publisher's Note: MDPI stays neutral with regard to jurisdictional claims in published maps and institutional affiliations.



Copyright: © 2022 by the authors. Licensee MDPI, Basel, Switzerland. This article is an open access article distributed under the terms and conditions of the Creative Commons Attribution (CC BY) license (<https://creativecommons.org/licenses/by/4.0/>).

1. Introduction

With the rapid development of the economy and technology, the pace of urbanization continues to accelerate. There are more and more skyscrapers and dense building groups in the city, due to the shortage of land resources. This trend influences the regional outdoor wind environment and causes a series of wind environment problems, such as strong winds, endangering safety, and reducing pedestrians' comfort [1–3]. Reports about pedestrians being blown down or fatally injured by strong winds are very common nowadays. In some cases, windows are blown off, causing property damage or casualties. The improper outdoor wind environment may cause local whirlpools and dead corners of airflow, hindering the pollutant diffusion and leading to human health problems [2–5]. The wind environment problems caused by poor-designed building layouts may also increase the energy consumption. In the summer, the air conditioning load increases, due to poor air circulation, while heating energy consumption soars, due to the high air permeability of the envelope structure, in the winter [6–8]. Therefore, for new buildings exceeding a certain height, the wind environment evaluation around the building is a must in many countries [9]. According to the assessment standard for China's green buildings,

the pedestrian height's wind speed limit around the building is five meters per second [10]. Therefore, the research and evaluation of the wind environment around a building can help optimize the architectural design and regional planning, which is crucial for creating a safe, comfortable, and healthy outdoor building environment and significant for building energy savings.

Computational fluid dynamic (CFD) simulations and wind tunnel experiments are popular methods to study and evaluate the outdoor wind environment [11,12], and they are widely used in architectural design. As a simple and fast method, a CFD simulation can obtain abundant data at a low cost [13–17]. However, it is greatly influenced by the turbulence models adopted and the user's experience. The calculation results vary from person to person, with great uncertainty [18]. Unlike the CFD method, the wind tunnel experiment is more reliable [11,18]. The advantages of this method include controllable airflow and boundary conditions, convenient measurement, stability in different climatic conditions, and reliable data output. Therefore, wind tunnel experiments are one of the most important and robust research methods in wind engineering [19–26]. For outdoor building environment measurements in a wind tunnel, it is important to simulate the real wind field in which the building is located. The atmospheric boundary layer (ABL), which is the layer at the bottom of the atmosphere, is greatly affected by the ground surface [27]. In particular, unlike wind engineering, which is concerned with the characteristics of the ABLs, the study of outdoor building environments pays more attention to the wind speed outside of the building under the common conditions in different seasons and the impact on the building ventilation and energy consumption, rather than on extreme environments [28]. Thus, this paper focuses on the wind speed created by the wind tunnel and will preliminarily discuss its applicability in the outdoor building environment research.

Spire and roughness elements are generally applied to the existing wind tunnel to create the gradient wind of the atmospheric boundary layer. When the terrain changes, the spires and roughness elements should be replaced or adjusted, correspondingly, to achieve the required airflow. Although the gradient wind formed by this wind tunnel is usable, the method is both time-consuming and labor-intensive. There are disadvantages, such as the large size, large footprint, as well as the higher cost of operation and maintenance [29,30]. The dimensions of the traditional low-speed wind tunnels, mentioned in the references [31–33], are about 12–24 m in length, 2–4 m in width, and height. In order to make the wind tunnel test more convenient and to reduce the footprint, some scholars adopted different methods to create the atmospheric gradient wind. Lloyd proposed three ways to create gradient wind [34]. Phillips used variable-spacing flat grids to simulate the wind speed profile and turbulence in the atmospheric boundary layer [35], then Yang et al. compared the wind field characteristics created by the five flat grids in a short test section [36]. In the design of the wind erosion wind tunnel, Pietersma and Fan used a honeycomb and screen, and Wu used a rod grid, and a roughness element method to construct the gradient wind [37–39]. Hlevca et al. and Pires et al. used rectangular grids, spires combined with blankets and screens, to create an atmospheric boundary layer in a small-scale wind tunnel, and further explored the atmospheric boundary layer construction method of a shorter-test segment wind tunnel, than in the previous study [40,41]. In this paper, unequally-spaced grids will be used to create the gradient wind of the atmospheric boundary layer. Compared with the theoretical values, the accuracy of this new compact wind tunnel is verified. With the application in an actual super high-rise building, the accessibility of this wind tunnel, applied to the study of the outdoor wind environment, is demonstrated.

2. Gradient Wind Model

The creation of the atmospheric boundary layer is the basis of the wind tunnel experiment, and it must be ensured that the atmospheric boundary layer is similar to that of the actual landforms, which is the key issue of the wind tunnel platform. The wind speed in the atmospheric boundary layer is a function of the height. According to the current

national standard for the wind tunnel tests of buildings and structures in China [42], an exponential law is used to characterize the relationship between the wind speed and the altitude in the boundary layer, as shown in Figure 1. The formula is as follows,

$$V_z = V_{10} \left(\frac{z}{10} \right)^\alpha \quad z_g \geq z \geq z_b \quad (1)$$

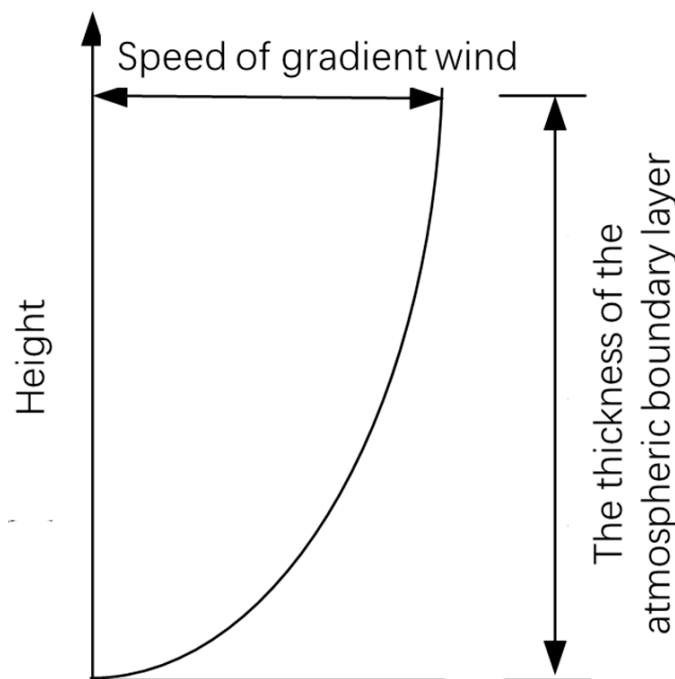


Figure 1. Schematic diagram of the gradient wind.

V_z : the average wind speed at height z , m/s.

V_{10} : the average wind speed at the height of 10 m, m/s.

z : the vertical height from the ground, m.

α : the wind speed profile index has different values according to the ground roughness category.

z_g : the gradient wind height, m.

z_b : the height of the starting profile, m.

According to the different surface roughness, landforms are clarified into four types, which are open space (A), town (B), urban (C), and high-rise building area (D). These four landforms' corresponding wind speed profile indexes are 0.12, 0.15, 0.22, and 0.30, respectively, with a boundary layer thickness of 300 m, 350 m, 450 m, and 550 m.

3. Wind Tunnel Platform

The compact wind tunnel platform was located at the building environment laboratory of Beijing Union University. The wind tunnel was made of plexiglass, with a dimension of 5 m (L) \times 1.2 m (W) \times 1.2 m (H), which was much smaller than the regular wind tunnel used for the building-wind-load measurement. It consisted of four parts along the airflow direction: the air supply segment, uniform flow segment, test segment, and air exhaust segment, as shown in Figure 2.

In the air supply segment, two symmetrical inlets with a diameter of 300 mm were set in the middle position of the left and right sides, to access the air supplied by the fan to the wind tunnel. Applying this air supply method, the air supply segment functioned as a plenum chamber, which can reduce the influence of the momentum of the incoming flow on the uniformity. In order to improve the uniformity of the airflow, a uniform flow segment was set behind the air supply segment. The length of this part was 2 m and consisted of

two plates. Holes with a diameter of 30 mm were evenly distributed on the first plate, and holes with a diameter of 10 mm for the second one. The distance between the two plates was 1 m. The plate with larger holes was placed in front, 0.5 m away from the center of the air supply outlet. In order to create the gradient wind of the atmospheric boundary layer, a grid plate with unequal spacing was set, which was 2.5 m away from the inlet, as shown in Figure 3. Based on Bernoulli’s equation and the equation for the local resistance of fluid flowing through the grid plate, the unequal spacing of the grid plate for four typical landforms could be calculated, respectively, to achieve the corresponding gradient wind. The different heights between the centerline and bottom plate a and the widths of each grill opening b, in Figure 3, are listed in Table 1. The test segment was behind the grid plate, where the building model is placed, and the outdoor wind environment was measured. At the end of the wind, the tunnel platform was the air exhaust segment, where the air was discharged.

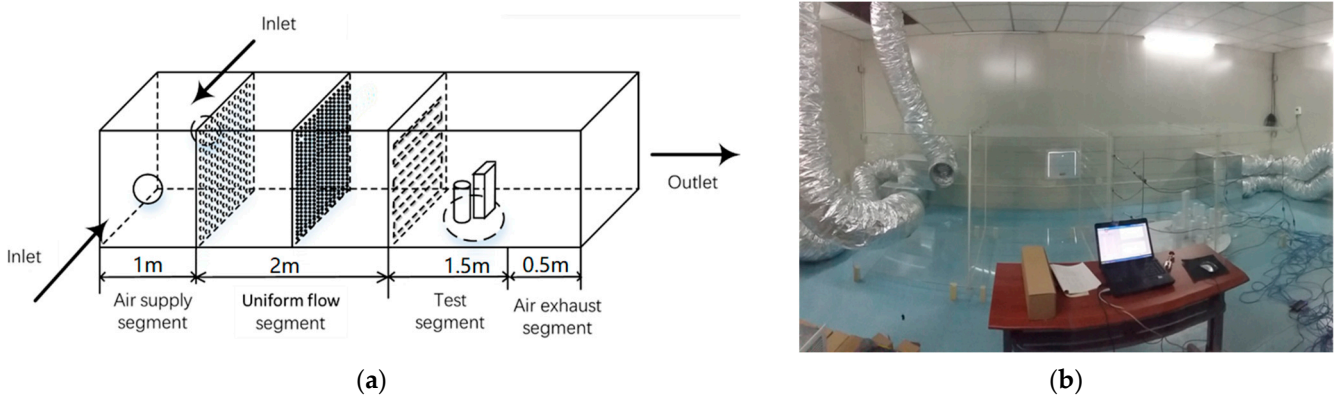
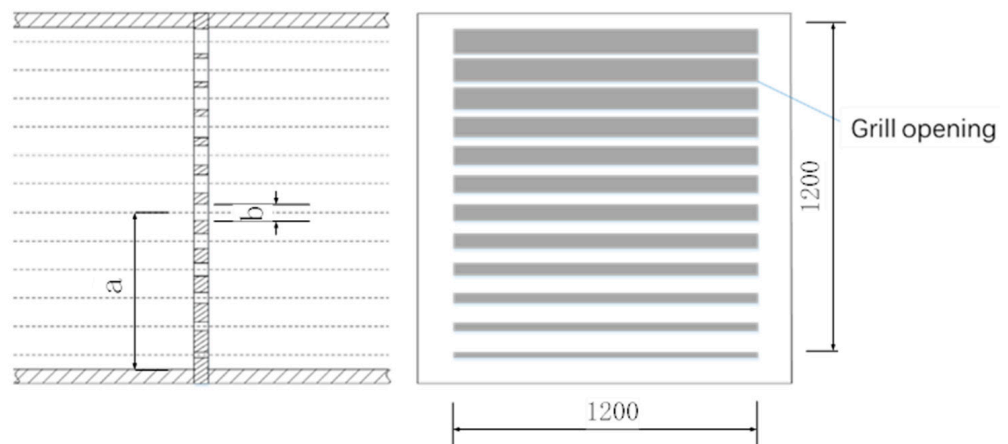


Figure 2. The wind tunnel platform. (a) Diagram of the platform; (b) Picture of the platform.



a: Height from the center line of the grid to the ground
 b: Height of the grid

Figure 3. Schematic diagram of a grid plate with unequal spacing (unit: mm).

Table 1. Dimensions of the grill openings of the grid plate.

a (mm)	50	150	250	350	450	550	650	750	850	950	1050
b (mm)	20	30.3	38.7	45.9	52.5	58.6	64.3	69.6	74.7	79.6	84.3

4. Performance Evaluation and Discussion

4.1. Measuring Method

A SWEMA 03 universal digital hot wire anemometer was used to measure the wind speed. The minimum response wind speed of the instrument was 0.03 m/s, the accuracy was $\pm 3\%$, the response time was less than 0.2 s, and the sampling frequency was 100 Hz. Multiple anemometers were used in the measurement. The anemometers were connected to the computer through a USB hub, to form a multipoint wind-speed data acquisition system. The wind speed was measured and recorded every 2 s, and the measurement lasted for 3 min. Finally, the arithmetic mean value of the collected wind speed was calculated as the wind speed of the measuring point.

4.2. Uniformity of the Wind Speed before the Grid Plate

Two cases with different air supply volumes, 5000 m³/h (case 1, the corresponding frequency of the air supply fan is 50 Hz) and 3680 m³/h (case 2, the corresponding frequency of the air supply fan is 35 Hz), were conducted, respectively. Four sections of 2 m, 2.5 m, 3 m, and 4 m away from the air supply inlet, were selected to evaluate the wind tunnel's uniformity of the wind speed before the grid plate. Nine measurement points were arranged regularly in each section, and there was a certain distance between the instrument and the wall, to minimize the measurement errors, as shown in Figure 4. Figures 5 and 6 present the measured wind speed values of each point on the different sections in the two cases. The relative deviation of the wind speed on different sections was calculated and shown in Figure 7.

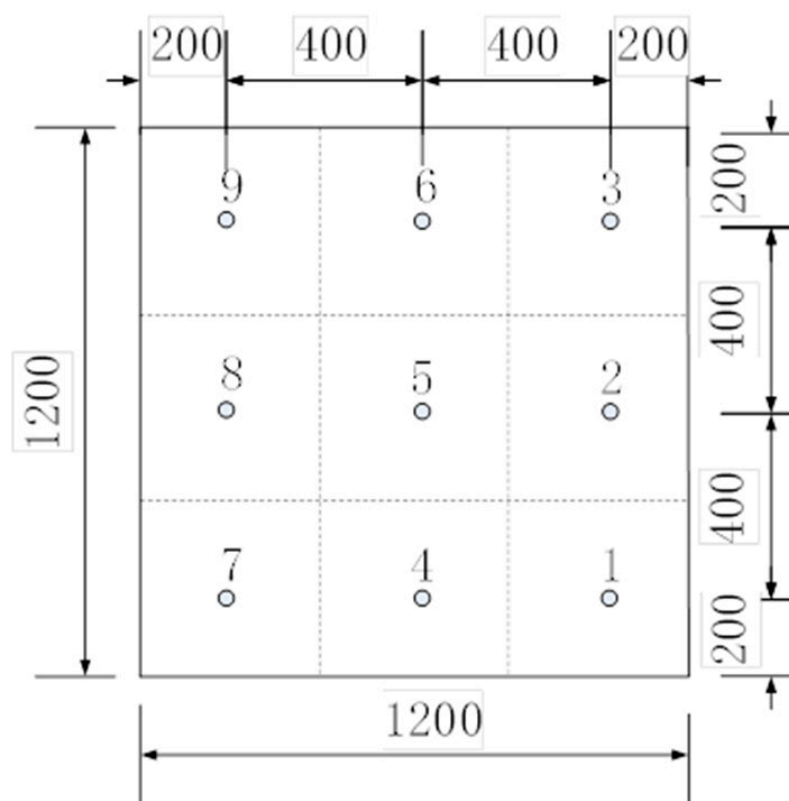
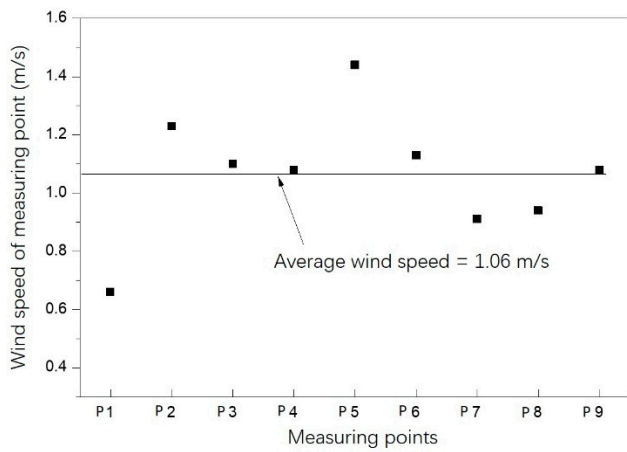
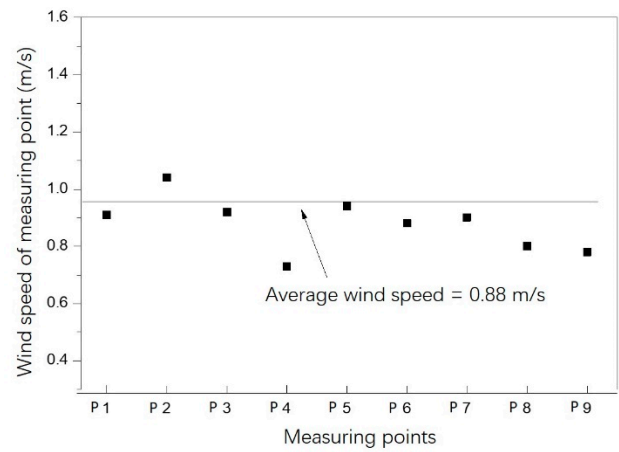


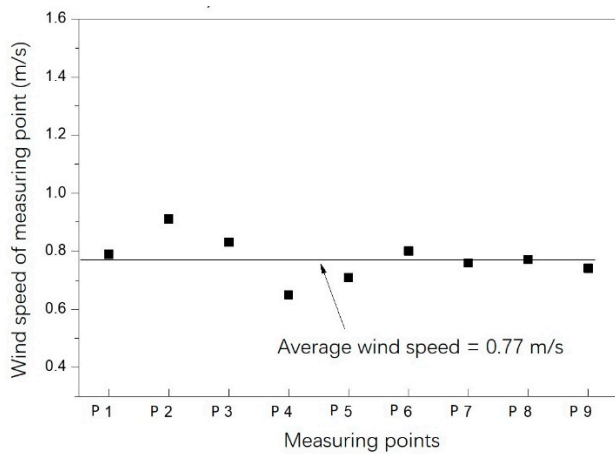
Figure 4. Arrangement of the nine measurement points of the section (unit: mm).



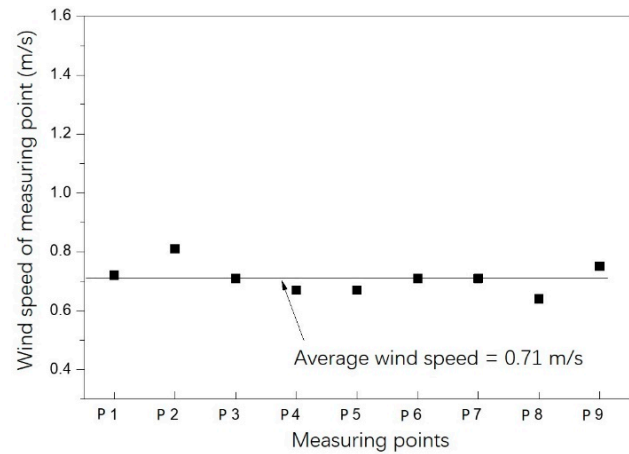
(a)



(b)

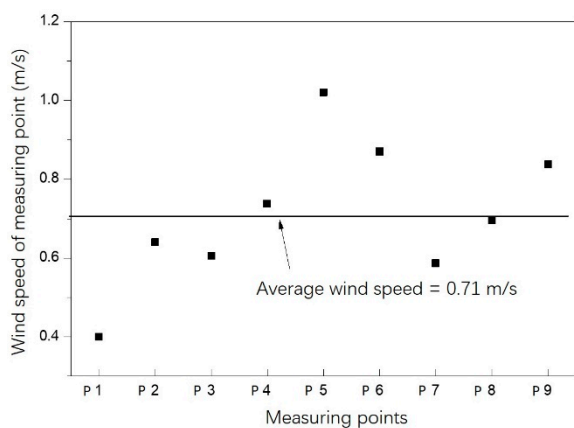


(c)

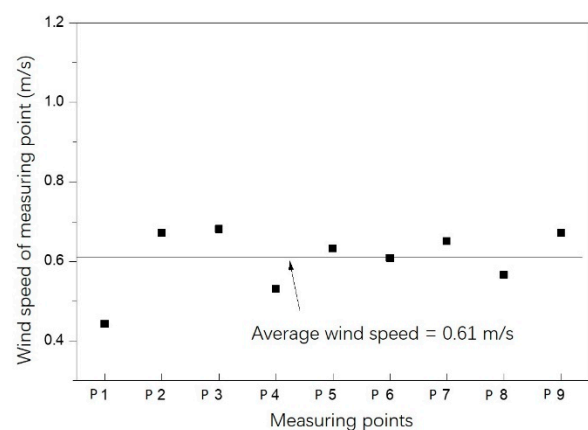


(d)

Figure 5. Wind speed of the measuring points on the different sections (case 1). (a) 2 m away from the air supply inlet; (b) 2.5 m away from the air supply inlet; (c) 3 m away from the air supply inlet; (d) 4 m away from the air supply inlet.



(a)



(b)

Figure 6. Cont.

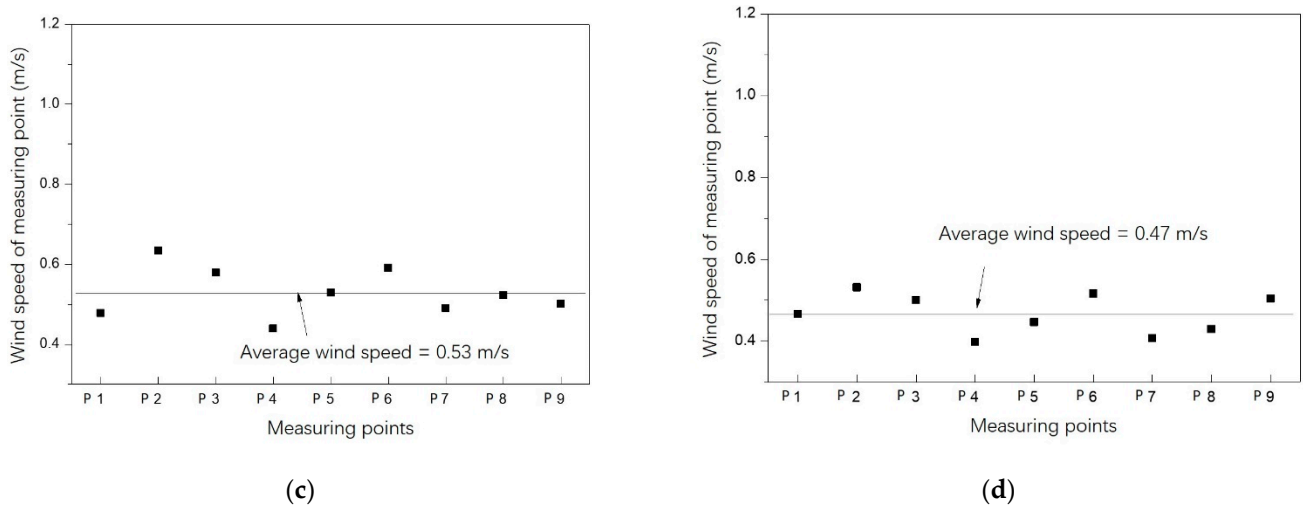


Figure 6. Wind speed of the measuring points on the different sections (case 2). (a) 2 m away from the air supply inlet; (b) 2.5 m away from the air supply inlet; (c) 3 m away from the air supply inlet; (d) 4 m away from the air supply inlet.

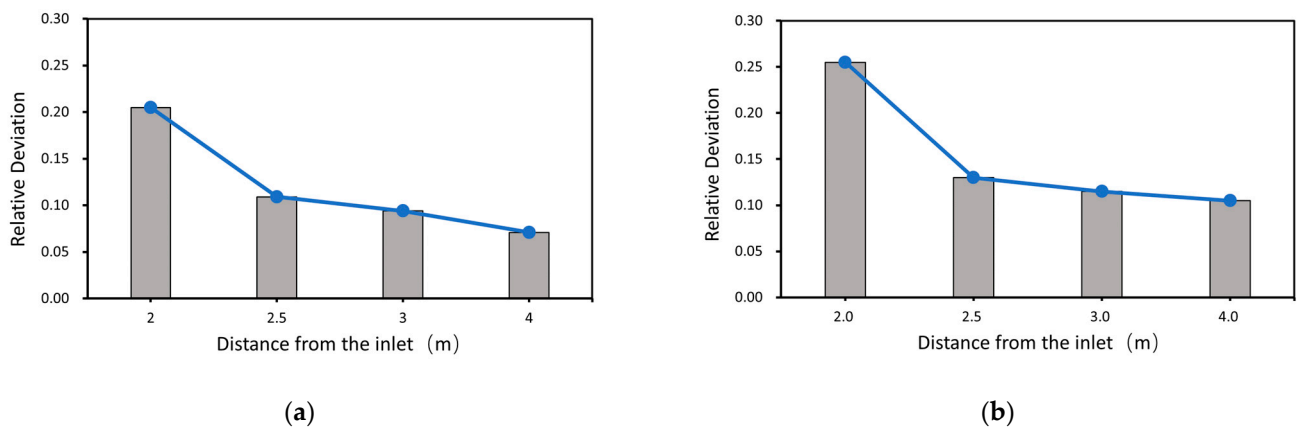


Figure 7. The relative deviation of the wind speed on the different sections. (a) case 1; (b) case 2.

As shown in Figures 5 and 7a, in case 1, the average wind speed of the measurement points on the section 2 m away from the air supply inlet was 1.06 m/s, and the maximum wind speed was 1.13 m/s. The minimum wind speed was 0.66 m/s, the standard deviation was 0.22 m/s, the relative deviation was 20.5%, and the COV value was 0.208. On the section 2.5 m from the air supply inlet, the average wind speed was 0.8 m/s, the maximum wind speed was 0.94 m/s, the minimum wind speed was 0.73 m/s, the standard deviation was 0.09 m/s, the relative deviation was 10.9%, and the COV value is 0.091. On the section 3 m away from the inlet, the average wind speed was 0.77 m/s, the maximum wind speed was 0.91 m/s, the minimum wind speed was 0.71 m/s, the standard deviation was 0.07 m/s, the relative deviation was 9.4%, and the COV value is 0.112. On the section 4 m away from the air inlet, the average wind speed decreased to 0.71 m/s, the maximum wind speed was 0.81 m/s, the minimum wind speed was 0.64 m/s, the standard deviation was 0.05 m/s, the relative deviation was 7.1%, and the COV value was 0.070. The comparison between the results of the different sections shows that the optimal distance was 4 m from the air supply inlet, where the standard, relative, and COV deviations were both the minimum. This implied the best uniformity of the wind speed. It also indicated that the uniformity of the wind speed is positively related to the distance from section to inlet. The same conclusion could also be drawn from the test results of case 2, as shown in Figures 6 and 7b. Figures 5 and 6 also indicate that, due to the wall resistance and the wind tunnel sealing, the average wind speed of the cross-section decreased with the distance. Considering the

characteristics of self-preservation of the wind field, the building model should be placed closer to the grid plate during the measurement, so that the wind speed of the wind tunnel matches the actual outdoor wind.

Comparing Figure 5 with Figures 6 and 6a with Figure 7b, it could be found that when the air supply volume increases, the relative deviation decreases or the uniformity of the wind speed improves.

4.3. Vertical Distribution of the Wind Speed behind the Grid Plate

As shown in Equation (1) and Figure 1, the gradient wind speed in the atmospheric boundary layer varied with the altitude. The purpose of this wind tunnel was to create a gradient wind field close to the theoretical curve. Therefore, whether the vertical distribution of the velocity behind the grid plate forms a gradient wind, is important; it is also a key index to evaluate the reliability of the wind tunnel.

According to the similarity criterion, the reference wind speed at the height of 10 m above the ground at the atmospheric boundary can be calculated, as shown in Equation (2) [43].

$$\frac{V_z}{V_R} = \left(\frac{z}{z_R}\right)^\alpha \quad (2)$$

V_z : the wind speed at height z , m/s.

V_R : the reference wind speed, m/s.

z_R : the reference height, m.

α : the average wind speed power index.

For case 1, the average wind speed of the uniform flow segment was 1.06 m/s, which was taken as the reference wind speed of the mainstream at the atmospheric boundary; thus V_{10} was 0.266 m/s, according to Equation (2).

For ease of comparison, the average wind speed of the different heights was converted into a wind speed ratio, as shown in Equation (3).

$$R_j = \frac{V_j}{V_{10}} \quad (3)$$

R_j : wind speed ratio at point j .

V_j : the average wind speed at point j , m/s.

According to Equation (3), the theoretical and measured wind speed ratios of the different heights can be calculated, respectively. The wind speed ratios of the two cases on the sections at the distance of 0.2 m and 0.5 m away from the grid plate are presented in Figure 8.

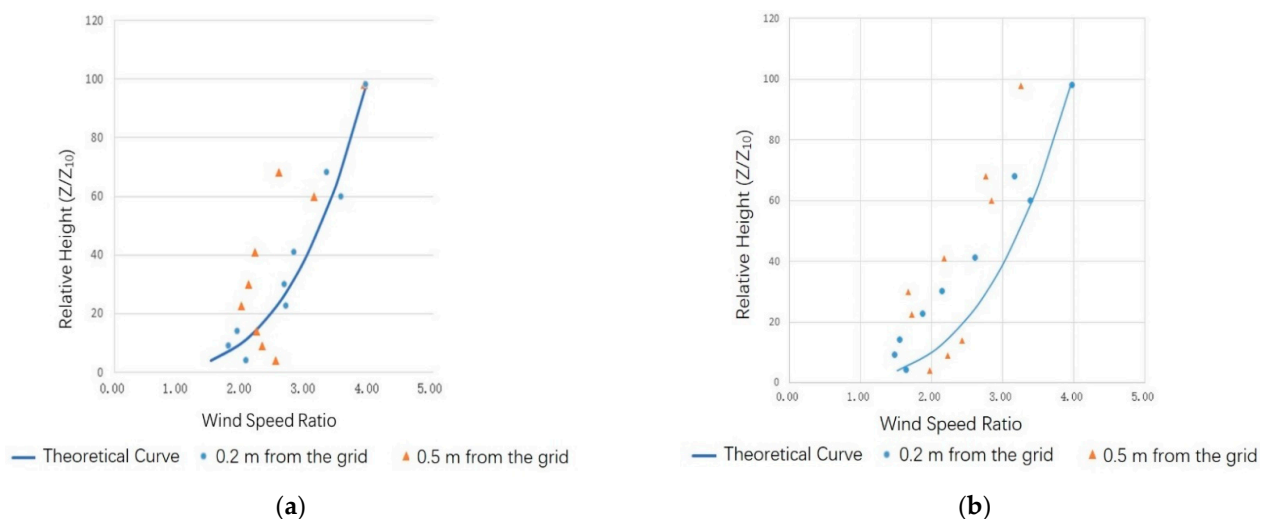


Figure 8. Comparison of the theoretical and measured wind speed ratios. (a) case 1; (b) case 2.

In Figure 8, for both cases, the wind speed ratio on the section of the distance of 0.2 m away from the grid plate is close to the trend of the theoretical target curve, which indicates that this wind tunnel can successfully form the gradient wind. The data of the measurement points with the vertical height ratio of 4 (the lowest measurement point) deviates farther from the target curve than the other points, which should be attributed to the short distance to the wall. By contrast, on the section 0.5 m away from the grid plate, the deviation of the measured value from the theoretical target curve increases. The increase is caused by the gradual attenuation of the wind speed and the reduction of the gradient difference.

Meanwhile, a comparison between Figure 8a,b shows that, as the air supply volume increases, the measurement value and the theoretical curve match better, which implies that the larger the supply air volume, the better the gradient wind can be obtained.

To investigate the wind tunnel's wall boundary's influence on the airflow, the wind speed near the wall was measured for case 1. The measuring points were arranged 0.1 m near the wall of the section. The wind speed of the section at 0.2 m and 0.5 m behind the grid plate, was measured, as shown in Figure 9. Compared with Figure 8, it can be seen that the wind speed near the wall at 0.2 m is also close to the theoretical curve. However, the wind speed of the different heights at 0.5 m, decreases significantly, and the deviation from the theoretical curve greatly increases, indicating that the wind speed gradient near the wall boundary cannot be consistent with the central mainstream. Therefore, when using this wind tunnel platform for testing, it is recommended that the building model be placed in the central mainstream area of the wind tunnel airflow.

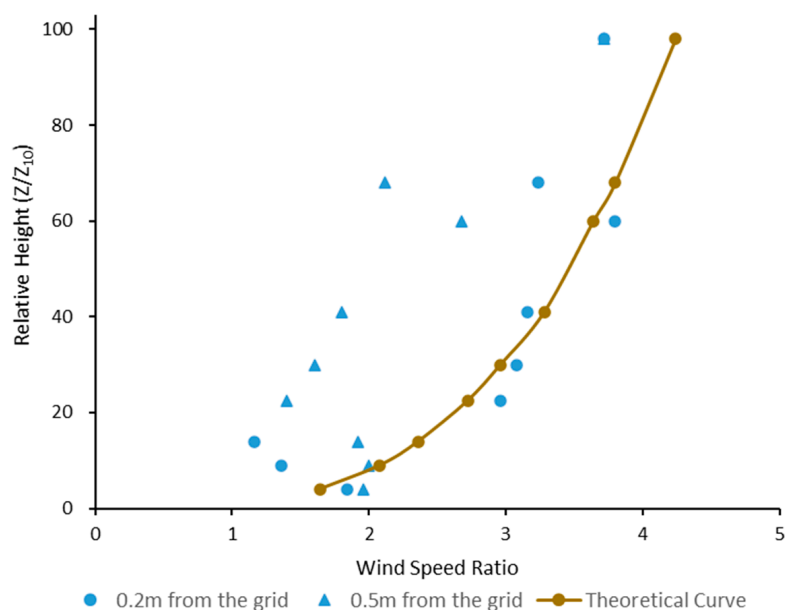


Figure 9. Comparison of the theoretical and measured wind speed ratios of the points near the wall boundary (case 1).

4.4. Retentivity of the Gradient Wind behind the Grid Plate

The distance the gradient wind behind the grid plate can maintain, is important, which will also determine where the building model should be placed in the practical application test. According to the above experimental data, taking the measurement data of the supply air volume of 5000 m³/h as an example, the measurement value of the wind speed ratio on different sections from the grid plate, was compared with the theoretical value, which was calculated by Equation 2, as shown in Figure 10.

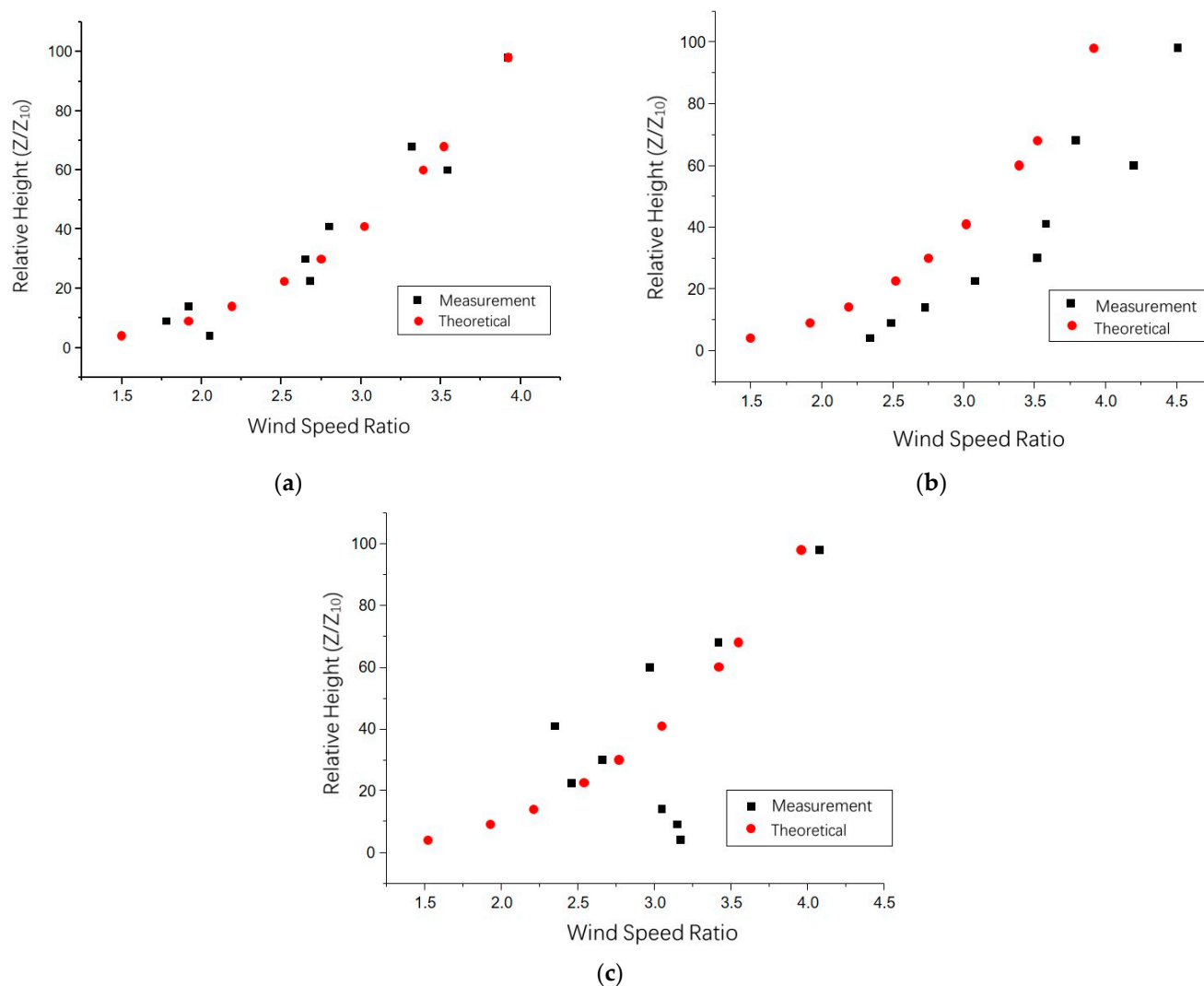


Figure 10. Average wind speed of the different sections behind the grid plate ($5000 \text{ m}^3/\text{h}$, 50 Hz). (a) 0.2 m away from the grid plate; (b) 0.5 m away from the grid plate; (c) 1.5 m away from the grid plate.

In Figure 10a, the measurement data of the section, which was 0.2 m away from the grid plate, was very close to the theoretical curve trend, indicating that it is accessible to create a gradient wind through different spacing grids. It can be seen from Figure 10b,c that the deviation between the measurement data and the theoretical curve of section 0.5 m away from the grid plate, gradually increases, and the deviation from the grid plate is further increased at the 1.5 m section. This shows that the stability and approximation of the gradient wind field decrease, were negatively proportional to the distance from the grid plate, which may be caused by the gradual attenuation and mixing of the wind speed. It also indicates that for the measurement points with relatively small vertical heights, or the points near the ground surface, the deviation of the measurement data from the theoretical curve is greater than that of the above points, which should be related to the roughness of the actual ground, which is difficult to simulate, accurately. For case 1, the characteristics of the wind field on the section of the distance 0.2 m away from the grid plate is optimal, which can prove that the wind tunnel successfully creates the wind profile under this condition. In contrast, the results are not ideal for other conditions. Therefore, it indicates that this experimental platform can qualitatively assess the pedestrian wind environment and is more suitable for studying and evaluating the overall wind environment outside of the building.

5. Application

5.1. Test Building and Model

The building tested in this paper was the CITIC Tower, a super high-rise building with a height of 528 m, located in the core area of Beijing's CBD, also known as 'China Zun', which is the tallest building in Beijing, surrounded by many skyscrapers. The numerous tall buildings in the CBD have significantly changed the regional wind environment, undermined the city's ventilation and self-cleaning capabilities, and exacerbated the city's air pollution and heat island effect under low wind speed conditions. Moreover, when the wind speed is high, there will be strong local winds around the buildings, affecting the comfort and safety of pedestrians.

In this paper, the wind tunnel platform mentioned above was used to conduct the experiments of the outdoor wind environment around 'China Zun' and the core area of the CBD to provide suggestions for the regional planning and architectural design. The architectural model was made of rigid materials with a scale of 1:1000, as shown in Figure 11. The diameter of the test model was 1.1 m, and the height of the 'China Zun' model was 52.8 cm. The building model was placed in the central mainstream area of the test segment's airflow, to minimize the wall boundary's influence. The maximum windward area is 0.13 m² of the three test conditions, and the blockage rate is 9.02%. According to the research by Hunt, the maximum allowable blockage rate is 10% for the wind speed measurement, using this kind of wind tunnel [44]. Considering the self-preservation of the wind field, the front point of the building model facing the incoming wind flow was 0.2 m away from the grid plate, which was 2.7 m away from the air supply inlets. Twenty test points were arranged in the horizontal direction to accurately obtain the wind speed distribution characteristics around the buildings and the changing trend in the boundary area of the air duct, as shown in Figure 11. The height of all of the test points was 2 cm (corresponding to the actual height of 20 m).

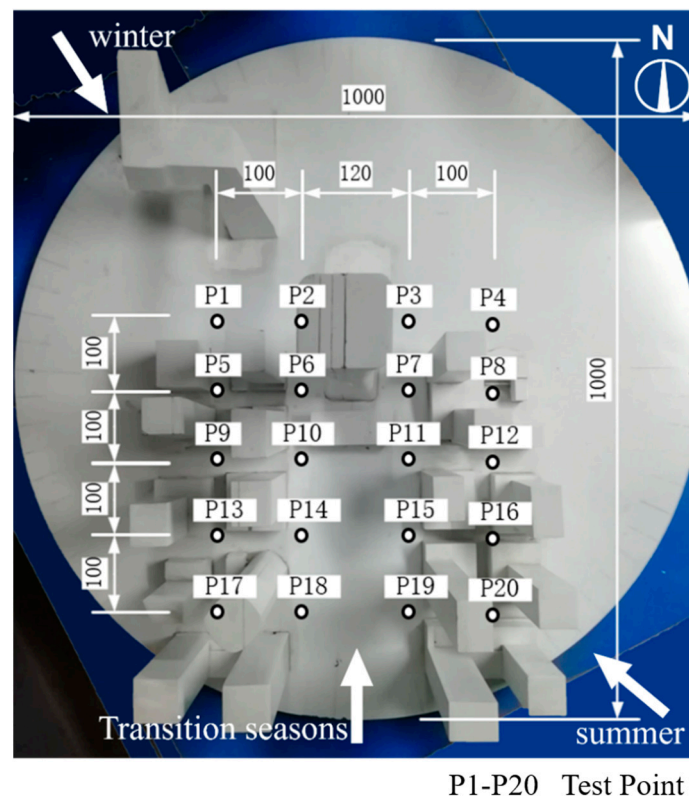


Figure 11. Building model and test points location (unit: mm).

5.2. Results and Analysis

The outdoor wind environment around the buildings under the dominant wind direction and the average wind speed of the winter, summer, and transition seasons, was tested. The measuring method used was described above. According to the meteorological data of Beijing, the wind direction of the winter test condition is northwest, with a wind speed of 2.7 m/s. The summer test condition wind direction is southeast with a wind speed of 2.2 m/s, and the transition season's wind direction is south with a wind speed of 2.5 m/s. The test results are shown in Figure 12.

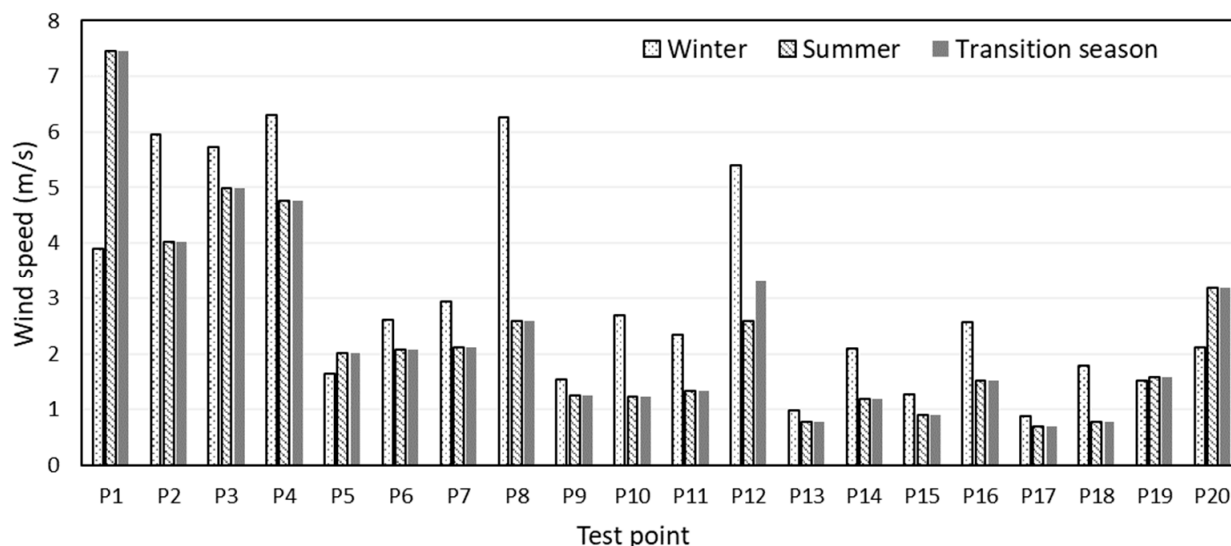


Figure 12. The wind speed of each test point in the different seasons.

In the winter test condition, the average wind speed of the test points was 3.03 m/s, and the wind field was non-uniform. Compared with the outside airflow wind speed, the core area's wind speed is significantly amplified, indicating that the super high-rise building hurts the urban wind environment.

In the summer and transitional season test conditions, the average wind speed of the test points was 2.66 m/s and 2.39 m/s, respectively. The wind fields were still non-uniform but had improved, compared to the winter. The reason is that the direction of the outside airflow was southeast and south. Therefore, there had no obvious channel effect, due to the lack of dense super high-rise buildings in these directions.

The test results are reasonable, indicating that this compact wind tunnel platform can be used to test, predict, and evaluate the outdoor wind environment around the building.

5.3. Comparison with the CFD Simulation

The measurement results are compared with a CFD simulation to validate the applicability of this compact wind tunnel in a building environment study. The CFD simulation of this paper was calculated using the PHOENICS software with a standard $k-\epsilon$ turbulence model. The data calculated by the CFD simulation method for the wind environment around the building has been validated for accuracy and has been used to verify the applicability of the volume particle tracking velocity (VPTV) measurement [45,46].

Considering that the purpose of the comparison was to validate the applicability of the compact wind tunnel platform, the inlet airflow boundary condition in the CFD calculation was determined according to the meteorological parameters in the design code, consistent with the wind tunnel test. Therefore, the overall measurement error of the wind tunnel platform can be verified during the data comparison.

The physical model of the CFD simulation was the CITIC Tower area, in the measurement of this paper. The orthogonal structured grids were used for the dispersion, and the total number of grids was about 0.3 million. The difference scheme was a power law

scheme, and the SIMPLE algorithm was adopted while momentum equations were solved on non-uniform staggered grids [47].

The air velocity distribution of the CFD calculation results for the winter and summer are shown in Figure 13, respectively. The comparison results, at the same location as the wind tunnel measurement, are shown in Figures 14 and 15. It can be seen that the average values of the measuring points in the winter and summer were close to the CFD calculation results; the wind tunnel measurement has a general rationality. Meanwhile, the relative errors of each measuring point were quite different. The maximum relative error in the winter was at P8, with an error of 83.36%. While the summer was at P18, with an error of 78.87%. The average relative error of each measuring point was 36.38% (winter) and 46.63% (summer), respectively. Combined with the wind tunnel inlet flow data in this paper, the inlet wind flow is relatively difficult with a high quality, which greatly impacts the building wind environment measurement.

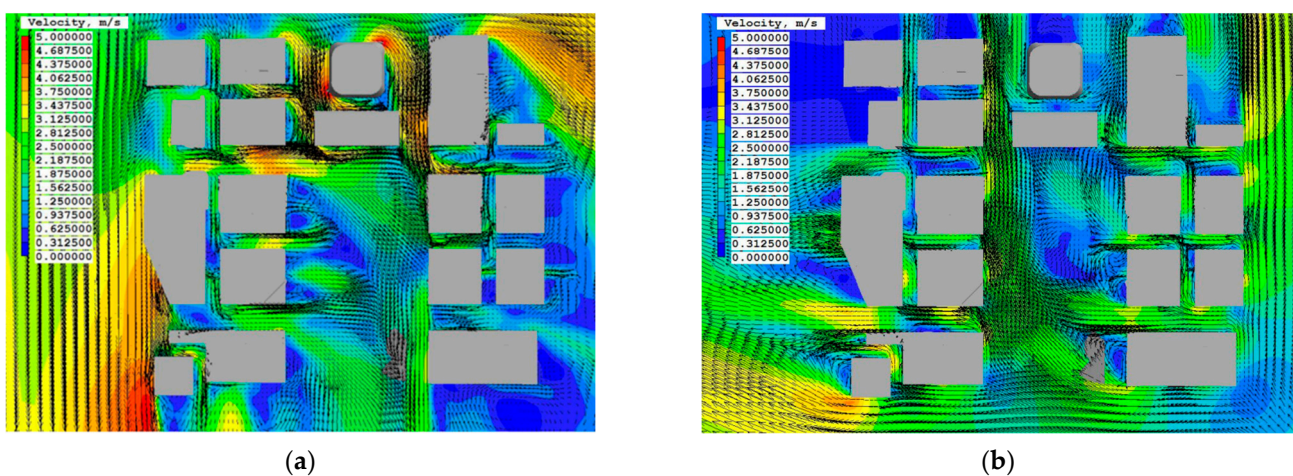


Figure 13. Air velocity distribution of the CFD simulation (plane view above-ground at 20 m). (a) winter; (b) summer.

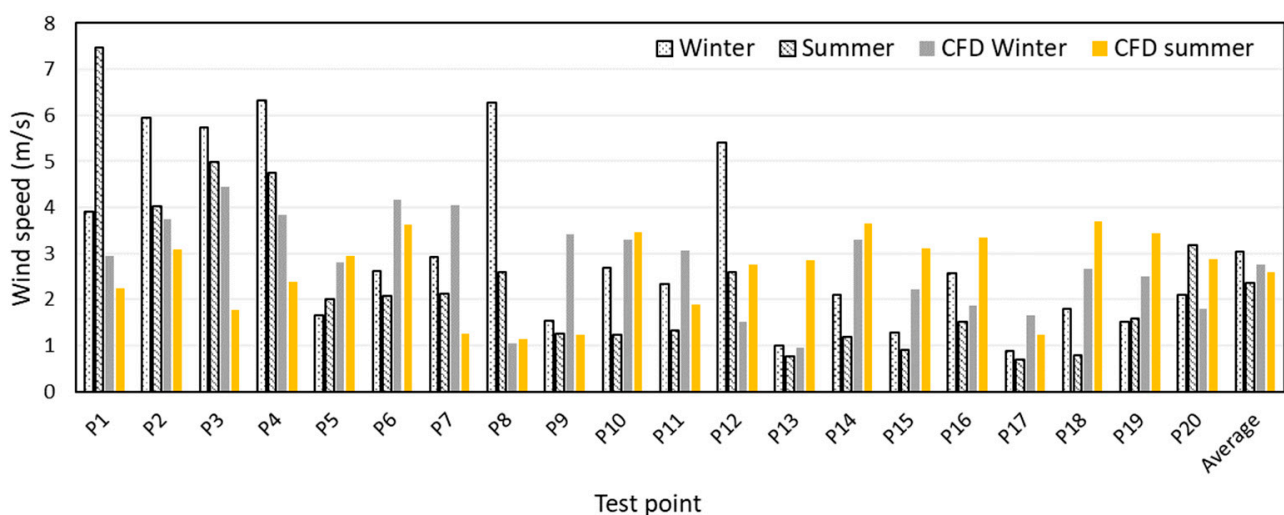


Figure 14. Wind speed comparison of the wind tunnel measurement and the CFD simulation.

Comparing the CFD simulation to the wind tunnel measurement, the applicability of this compact wind tunnel in the building environment study was validated. It indicates that the efficiency, effect, and cost of the compact wind tunnel and the CFD method are similar. Furthermore, the accuracy of the quality of the inlet flow needs to be improved.

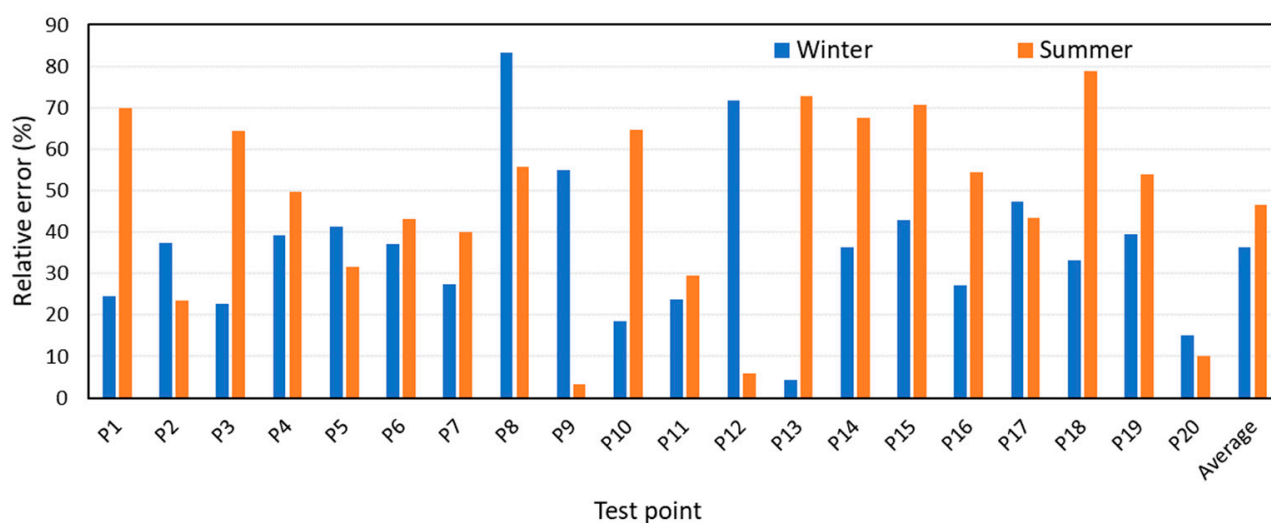


Figure 15. Relative errors of the wind speed data.

6. Conclusions

Wind tunnel experiments are an important method in studies on the outdoor wind environment. In this paper, a compact wind tunnel platform was designed, based on the theoretical model of the atmospheric boundary layer. In addition, grids with unequal spacing were adopted and tested. The comparison with the theoretical formula proved that this method could achieve the gradient wind. The application in the CBD region of Beijing indicated that it could be used to predict and evaluate the outdoor wind environment around the building. By comparing with the CFD method, it can be seen that this compact wind tunnel is reliable and accessible for the measurement and research of outdoor building wind environments under low wind speeds.

Compared to a large-scale wind tunnel, the compact wind tunnel platform in this paper is more flexible and convenient, with a smaller land occupation, easier construction, operation, and lower cost for the outdoor building wind environment research, with a low-speed airflow field. In addition, the research of this paper indicates that this compact wind tunnel still has some shortcomings, such as non-uniformity of the wind speed, a lower accuracy of the gradient wind, and some important parameters of the ABL. More applications of this compact wind tunnel under different conditions will be conducted in the future, and thick plates with unequal spacing will be adopted and compared with the grids method, to achieve a better gradient wind.

Author Contributions: Conceptualization, X.M. and J.C.; methodology, Y.Z. and X.M.; software, Y.Z.; validation, X.M., X.W. and J.C.; formal analysis, Y.Z. and X.W.; investigation, X.M., Y.Z. and X.W.; resources, X.M.; data curation, J.C. and X.W.; writing—original draft preparation, J.C.; writing—review and editing, X.M., Y.Z. and X.W.; visualization, Y.Z. and J.C.; supervision, X.M.; project administration, X.M.; funding acquisition, X.M. All authors have read and agreed to the published version of the manuscript.

Funding: This research was funded by the China National Key R&D Program, grant number 2018YFC0705204.

Data Availability Statement: Not applicable.

Conflicts of Interest: The authors declare no conflict of interest.

References

1. Lawson, T.V.; Penwarden, A.D. The effects of wind on people in the vicinity of buildings. In Proceedings of the 4th Wind Effects on Buildings and Structures, Heathrow, UK, 1975; pp. 605–622.
2. Stathopoulos, T. Pedestrian level winds and outdoor human comfort. *J. Wind Eng. Ind. Aerod.* **2006**, *94*, 769–780. [[CrossRef](#)]

3. Moonen, P.; Defraeye, T.; Dorer, V.; Blocken, B.; Carmeliet, J. Urban physics: Effect of the micro-climate on comfort, health and energy demand. *Front. Archit. Res.* **2012**, *1*, 197–228. [[CrossRef](#)]
4. Penwarden, A.D.; Wise, A. *Wind Environment around Buildings*; HM Stationery Office: London, UK, 1975.
5. Murakami, S.; Uehara, K.; Komine, H. Amplification of wind speed at ground level due to construction of high-rise building in urban area. *J. Wind Eng. Ind. Aerod.* **1979**, *4*, 343–370. [[CrossRef](#)]
6. Peter, F.S. *Architecture in a Climate of Change: A Guide to Sustainable Design*, 2nd ed.; Architectural Press: Boston, MA, USA, 2005.
7. You, W.; Shen, J.L.; Ding, W.W. Improving Wind Environment of Residential Neighborhoods by Understanding the Relationship between Building Layouts and Ventilation Efficiency. *Energy Procedia* **2017**, *105*, 4531–4536. [[CrossRef](#)]
8. Sakiyama, N.R.M.; Carlo, J.C.; Frick, J.; Garrecht, H. Perspectives of naturally ventilated buildings: A review. *Renew. Sust. Energy Rev.* **2020**, *130*, 109933. [[CrossRef](#)]
9. Shahrestani, M.; Yao, R.; Cook, G.K. A review of existing building benchmarks and the development of a set of reference office buildings for England and Wales. *Intell. Build. Int.* **2014**, *6*, 41–64. [[CrossRef](#)]
10. China Academy of Building Research. *Assessment Standard for Green Building*, 1st ed.; China Architecture & Building Press: Beijing, China, 2014.
11. Blocken, B.; Stathopoulos, T.; Beeck, J.P.A.J.V. Pedestrian-level wind conditions around buildings: Review of wind-tunnel and CFD techniques and their accuracy for wind comfort assessment. *Build. Environ.* **2016**, *100*, 50–81. [[CrossRef](#)]
12. Hemant, M.; Ashutosh, S.; Ajay, G. A review on the study of urban wind at the pedestrian level around building. *J. Build. Eng.* **2018**, *18*, 154–163.
13. Blocken, B.; Janssen, W.D.; Hooff, T.V. CFD simulation for pedestrian wind comfort and wind safety in urban areas: General decision framework and case study for the Eindhoven University campus. *Environ. Modell. Softw.* **2012**, *30*, 15–34. [[CrossRef](#)]
14. Mochida, A.; Lun, I.Y.F. Prediction of wind environment and thermal comfort at pedestrian level in urban area. *J. Wind Eng. Ind. Aerod.* **2008**, *96*, 1498–1527. [[CrossRef](#)]
15. Li, Y.; Chen, L. Study on the influence of voids on high-rise building on the wind environment. *Build. Simul.* **2020**, *13*, 419–438. [[CrossRef](#)] [[PubMed](#)]
16. Andrea, D.L.V.; Giuseppe, D.S.; Roberto, R.; Andrea, V. Numerical study of urban canyon microclimate related to geometrical parameters. *Sustainability* **2014**, *6*, 7894–7905.
17. Omar, S.A. Prediction of wind environment in different grouping patterns of housing blocks. *Energ. Build.* **2010**, *42*, 2061–2069.
18. Blocken, B. Computational fluid dynamics for urban physics: Importance, scales, possibilities, limitations and ten tips and tricks towards accurate and reliable simulations. *Build. Environ.* **2015**, *91*, 219–245. [[CrossRef](#)]
19. Tsang, C.W.; Kwok, K.C.S.; Hitchcock, P.A. Wind tunnel study of pedestrian level wind environment around tall buildings: Effects of building dimensions, separation and podium. *Build. Environ.* **2012**, *49*, 167–181. [[CrossRef](#)]
20. Stabile, L.; Arpino, F.; Buonanno, G.; Russi, A.; Frattolillo, A. A simplified benchmark of ultrafine particle dispersion in idealized urban street canyons: A wind tunnel study. *Build. Environ.* **2015**, *93*, 186–198. [[CrossRef](#)]
21. Niachou, U.K.; Livada, I.; Santamouris, M. Experimental study of temperature and airflow distribution inside an urban street canyon during hot summer weather conditions. Part II: Airflow analysis. *Build. Environ.* **2008**, *43*, 1393–1403. [[CrossRef](#)]
22. Ricci, A.; Burlando, M.; Freda, A.; Repetto, M.P. Wind tunnel measurements of the urban boundary layer development over a historical district in Italy. *Build. Environ.* **2017**, *111*, 192–206. [[CrossRef](#)]
23. Weerasuriya, A.U.; Tse, K.T.; Zhang, X.L.; Li, S.W. A wind tunnel study of effects of twisted wind flows on the pedestrian level wind field in an urban environment. *Build. Environ.* **2018**, *128*, 225–235. [[CrossRef](#)]
24. Zhang, X.L.; Tes, K.T.; Weerasuriya, A.U.; Li, S.W.; Kwok, K.C.S.; Mak, C.M.; Niu, J.L.; Lin, Z. Evaluation of pedestrian wind comfort near “lift-up” buildings with different aspect ratios and central core modifications. *Build. Environ.* **2017**, *124*, 245–257. [[CrossRef](#)]
25. Du, Y.; Mar, C.M.; Kwok, K.; Tse, K.M.; Lee, T.C.; Ai, Z.T.; Liu, J.L.; Niu, J.L. New criteria for assessing low wind environment at pedestrian level in Hong Kong. *Build. Environ.* **2017**, *123*, 23–36. [[CrossRef](#)]
26. Antoniou, N.; Montazeri, H.; Wigo, H.; Neophytou, M.K.A.; Blocken, B.; Sandberg, M. CFD and wind tunnel analysis of outdoor ventilation in a real compact heterogeneous urban area: Evaluation using “air delay”. *Build. Environ.* **2017**, *126*, 355–372. [[CrossRef](#)]
27. Cai, J.H.; Zhao, P.; Shi, Q.; Yang, Q.Y. Research progress in atmospheric boundary layer. *Chin. J. Geophys.* **2021**, *64*, 735–751.
28. Durgin, F.H. Pedestrian level wind studies at the Wright brothers facility. *J. Wind Eng. Ind. Aerod.* **1992**, *44*, 2253–2264. [[CrossRef](#)]
29. Counihan, J. An Improved Method of Simulating an Atmospheric Boundary Layer in a Wind Tunnel. *Atmos. Environ.* **1969**, *3*, 197–214. [[CrossRef](#)]
30. Cesar, F.; Arun, K.S.I. Experiments on the wind tunnel simulation of atmospheric boundary layers. *J. Wind Eng. Ind. Aerod.* **1999**, *79*, 11–35.
31. Feng, S.; Wang, Y.; Xie, Z. Estimating extreme wind pressure for long-span roofs: Sample independence considerations. *J. Wind Eng. Ind. Aerod.* **2020**, *205*, 104341. [[CrossRef](#)]
32. Han, Z.; Li, B.; Tian, Y.; Xue, M.; Shao, S. Investigation of Wind-Loads Acting on Low-Aspect-Ratio Cylindrical Structures Based on a Wind Tunnel Test. *Appl. Sci.* **2022**, *12*, 5891. [[CrossRef](#)]
33. Blocken, B.; Stathopoulos, T.; Carmeliet, J. Wind environmental conditions in passages between two long narrow perpendicular buildings. *J. Aerosp. Eng.* **2008**, *21*, 280–287. [[CrossRef](#)]

34. Lloyd, A.R.J. The Generation of Shear Flow in a Wind Tunnel. *Q. J. R. Meteorol. Soc.* **1967**, *93*, 79–96. [[CrossRef](#)]
35. Phillips, J.C.; Thomas, N.H.; Perkins, R.J.; Hiller, P.C. Wind tunnel velocity profiles generated by differentially-spaced flat plates. *J. Wind Eng. Ind. Aerod.* **1999**, *80*, 253–262. [[CrossRef](#)]
36. Yang, J.W.; Yang, H.; Fu, S.F.; Zong, W.W.; Sha, C.L. Wind tunnel test study of grid turbulence field in short test section. *J. Exp. Fluid Mech.* **2021**, *35*, 86–93.
37. Pietersma, D.; Stetler, L.D.; Saxton, K.E. Design and aerodynamics of a portable wind tunnel for Soil erosion and fugitive dust research. *Trans. ASAE* **1996**, *39*, 2075–2083. [[CrossRef](#)]
38. Fan, G.S. Design and Aerodynamic Performance of Movable Wind Erosion Wind Tunnel. Ph.D. Thesis, Inner Mongolia Agricultural University, Hohhot, China, 2005.
39. Wu, L.P. Design and Development of Pneumatic Structure of NK-1 Movable Wind Erosion Wind Tunnel. Ph.D. Thesis, Nankai University, Tianjin, China, 2012.
40. Hlevca, D.; Degeratu, M. Atmospheric boundary layer modeling in a short wind tunnel. *Eur. J. Mech. B-Fluids* **2020**, *79*, 367–375. [[CrossRef](#)]
41. Pires, L.B.M.; Paula, I.B.D.; Fisch, G.; Gielow, R.; Girardi, R.D.M. Simulations of the Atmospheric Boundary Layer in a Wind Tunnel with Short Test Section. *J. Aerosp. Technol. Man.* **2013**, *5*, 305–314. [[CrossRef](#)]
42. China Academy of Building Research. *Standard for Wind Tunnel Test of Buildings and Structures*, 1st ed.; China Architecture & Building Press: Beijing, China, 2014.
43. Wind Tunnel Experiment Guide Research Committee; Sun, Y.; Wu, Y.; Cao, Z.G. *Guide to Architectural Wind Tunnel Experiments*; China Architecture and Architecture Press: Beijing, China, 2011. (In Japanese)
44. Hunt, A. Wind tunnel measurements of surface pressures on cubic building models at several scales. *J. Wind Eng. Ind. Aerod.* **1982**, *10*, 137–163. [[CrossRef](#)]
45. Zhao, Y.; Ma, X.; Zhang, C.; Wang, H.; Zhang, Y. 3D real-time volumetric particle tracking velocimetry—A promising tool for studies of airflow around high-rise buildings. *Build. Environ.* **2020**, *178*, 106930. [[CrossRef](#)]
46. Shao, J.; Liu, J.; Zhao, J. Evaluation of various non-linear k- ϵ models for predicting wind flow around an isolated high-rise building within the surface boundary layer. *Build. Environ.* **2012**, *57*, 145–155. [[CrossRef](#)]
47. Launder, B.E.; Spalding, D.B. The numerical computation of turbulent flows. *Comput. Methods Appl. Mech. Eng.* **1974**, *3*, 269–289. [[CrossRef](#)]